INFLUENCE OF FROST DAMAGE ON WATER PENETRATION INTO NEAT AND AIR ENTRAINED CONCRETE

Peng Zhang [1, 2*], Yanru Wang [1], Tiejun Zhao [1, 2], Jigang Zhang [1, 2] and Qing Liu [1]
[1] Department of Civil Engineering, Qingdao Technological University,
Qingdao 266033, PR China
[2] Center for Durability & Sustainability Studies of Shandong Province,
Qingdao 266033, PR China *Email:zhp0221@163.com

ABSTRACT

In service life, concrete can be damaged either by mechanical or environmental loads or by combined ones. These damages will strongly influence water movement in concrete which could later lead to more serious deteriorations. This paper applies neutron radiography to investigate the influence of frost damage on water penetration into concrete. In addition, the improvement of frost resistance by addition of air entrainment was investigated. The results indicate that it is possible to visualize penetration of water into the porous structure of concrete by neutron radiography. Further evaluation of the test data allows determining time-dependent moisture profiles quantitatively with high resolution. After concrete is damaged by freeze-thaw cycles water penetration into ordinary concrete is accelerated. It can be shown that frost damage is not equally distributed in specimens exposed to freeze-thaw cycles. Thermal gradients lead to more serious damage near the surface. The beneficial effect of air entrainment on frost resistance has been demonstrated. After 50 freeze-thaw cycles, air entrained concrete showed no measurable increase in water absorption. But layers near the surface of concrete absorbed slightly more water after 200 freeze-thaw cycles although the dynamic elastic modulus remained constant. Results presented in this paper help us to better understand mechanisms of frost damage of concrete.

KEYWORDS

Freeze-thaw cycles, concrete, water penetration, air entrainment, thermal gradient, moisture distribution, neutron radiography.

INTRODUCTION

Cracks are always preferential paths for water flow. Cracks may be caused by mechanical load or by thermal and hygral gradients or by local swelling processes. Many authors have studied the influence of cracks on penetration of water and aggressive compounds into cement-based materials in the past (see for example, Jacobsen et al. 1996; Aldea et al. 1999; Win et al. 2004; Kato et al. 2005; Yang et al. 2006; Wang et al. 2008; Kanematsu et al. 2009; Picandet et al. 2009). Jacobsen et al. (1996) studied the effect of freeze-thaw cycles on chloride transport into concrete and they found that internal cracking increased the chloride penetration rate by a factor of 2.5 to 8 when compared with undamaged specimens. Yang et al. (2006) studied water transport in concrete damaged both by tensile loading and frost cycles and reported that the presence of freeze-thaw damage increased both the initial sorptivity and total water absorption of concrete.

It is obvious that if one uses material properties measured on undamaged concrete in prediction models the performance of a structure in aggressive environment may be overestimated. There is an urgent need to modify existing prediction models in such a way that they can take into account mass transport properties modified by damage due to mechanical or environmental loads. But necessary experimental data to feed this new generation of models are scarce. By means of neutron radiography it is possible to visualize and quantify water penetration into concrete. Up to now, this technique has been successfully applied already to study water movement in different porous building materials such as concrete, mortar, stone, and bricks by several researchers (see for example: Pleinert et al. 1998; Lehmann et al. 2002; Hassanein et al. 2006; Cnudde et al. 2008; Abd et al. 2009; Zhang et al. 2010).

The main aim of this paper is to investigate the influence of freeze-thaw cycles on water penetration into

concrete. To which extend is capillary water absorption increased by damage induced by frost action? From the raw data obtained by neutron radiography time-dependent spatial water distributions in concrete during water penetration can be determined in a quantitative way. Frost damage usually is assumed to be equally distributed in the volume. It should be possible to observe additional damage near the surface due to hygral gradients during cooling. All results obtained will be presented and discussed.

MATERIALS AND METHODS

Materials and Preparation of Test Specimens

Prismatic specimens with the following dimensions were prepared with two types of concrete, both with water cement ratio of 0.6: 100 mm × 100 mm × 400 mm. Ordinary Portland cement type 42.5, local crushed aggregates with a maximum diameter of 20 mm and density of 2620 kg/m3, river sand with a maximum grain size of 5 mm and density of 2610 kg /m3, all from Qingdao area, were used. Part of the specimens was produced with the addition of 0.017 % of an air entraining agent related to the mass of cement into the fresh concrete to improve its frost resistance. The exact compositions of the two types of concrete C and CA used in this project, and their air content and compressive strength at an age of 28 days are given in Table 1.

Table 1: Composition, air content and compressive strength of two types of concrete used in this project.

Concrete Type	Cement (kg/m^3)	Sand (kg/m^3)	Gravel (kg/m^3)	Water (kg/m^3)	Air entraining agent (g/m^3)	Air content (%)	28-day compressive strength (MPa)
C	300	699	1191	180	—	2.0	32.2
CA	300	699	1191	180	51	5.2	28.9

All concrete specimens were demoulded after one day and then stored in a moist curing room at a temperature of 20 ± 3 ℃ and relative humidity higher than 95 % until an age of 24 days. At that time all specimens were taken out of the curing room and further stored in water for another four days. At an age of 28 days, specimens were then ready for the following frost test.

Freeze-thaw Cycles

After curing concrete specimens were exposed to freeze-thaw cycles following a Chinese standard method (2010). In this case one freeze-thaw cycle lasts for about three hours. The temperature at the centre of specimens varied between -17 ± 2 ℃ and 5 ± 2 ℃. On concrete samples without addition of air entraining agent (Concrete C), the dynamic elastic modulus has been measured after 10 and 25 freeze-thaw cycles. On concrete samples prepared with addition of air entraining agent (Concrete CA), the dynamic elastic modulus has been measured after 10, 50, 100, 150, 200, 250 and 300 freeze-thaw cycles. In the following, specimens which had suffered freeze-thaw cycles are identified by the appropriate concrete type followed by the number of frost cycles, as for instance, the concrete with air entrainment exposed to 200 freeze-thaw cycles will be designated “CA-200”. As can be expected concrete made with air entraining agent has a significantly improved frost resistance. Change of the related dynamic elastic modulus of both types of concrete, without and with air entraining agent, as function of number of frost cycles is shown in Figure 1.

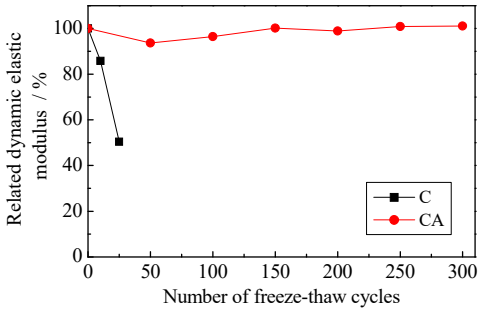

Figure 1 Related dynamic elastic modulus of two types of concrete C and CA as function of the number of freeze-thaw cycles

After exposure to a certain number of freeze-thaw cycles, selected specimens were taken out of the frost testing machine and cut in parts for water penetration tests. First a centre cube with dimensions with an edge length of 100 mm was cut off. Then two opposite layers with a thickness of 25 mm each were cut off the cube. Finally the remaining block which had the following dimensions: 100 mm × 50 mm × 100 mm has been separated into five thin slices with a thickness of approximately 20 mm. The cutting scheme is shown schematically in Figure 2. Slices from the surface were designated as “-1”, the intermediate slices with “-2” and the centre slice with “-3”.

The test sample were then dried in a ventilated oven at 50 ℃ for four days until constant weight was achieved. Then four surfaces were covered with self-adhesive aluminum foil. Two opposite surfaces with the dimensions 20 mm × 100 mm remained free for the capillary absorption test. After the first image had been taken by means of neutron radiography in the dry state of the specimens the aluminum container was filled with water. At this moment water started to penetrate into the frost damaged concrete. Neutron images were then taken at regular intervals following the process of water penetration into the samples. The obtained raw data were later evaluated by means of appropriate computer programs in order to determine time-dependent water distributions quantitatively.

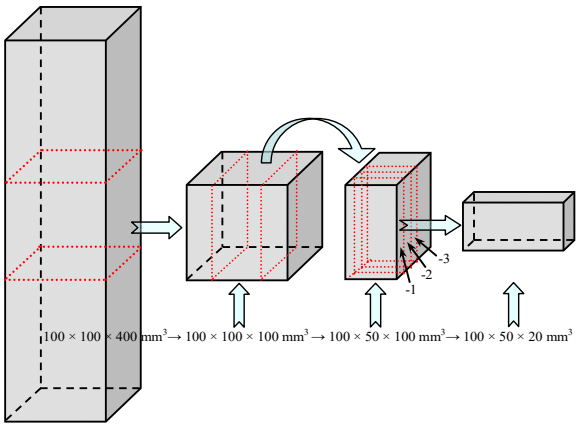

Figure 2 Schematic representation for cutting specimens

Neutron Radiography

All tests of neutron radiography were performed at the thermal neutron radiographic facility called NEUTRA of Paul Scherrer Institute (PSI) in Switzerland (Lehmann et al. 2002). The basic set-up of neutron radiography is shown in Figure 3. After the reservoir was filled with water neutron images were serially taken every twenty seconds for up to four hours. In order to visualize more clearly the process of water penetration into concrete, differential images from any time related to the initial time were then processed. For the quantitative evaluation of the digitized neutron radiographs, a software program was utilized. More details about quantitative calculation of water content in porous materials can be found in references (Pleinert et al. 1998; Hassanein et al. 2006; Abd et al. 2009; Zhang et al. 2009).

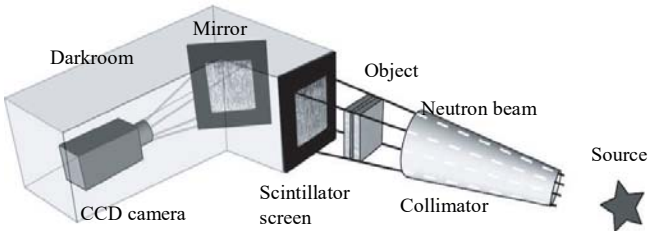

Figure 3 Basic set-up of neutron radiography

RESULTS AND DISCUSSION

Water Penetration into Concrete without Air Entrainment after Frost Damaged

Neutron images of water penetration into concrete without air entrainment and without frost action are shown in Figure 4. It can be seen immediately that by means of neutron radiography we can follow qualitatively the process of water penetration into porous cement-based materials. After a contact time of about five minutes the penetrating water front becomes visible. Then this irregular front gradually moves deeper into concrete with increasing contact time. The aggregates of the composite material are marked with the lighter areas as they do hardly absorb water. The water moves around the aggregates in the porous cement-based matrix. The time-dependent moisture profile along a vertical axis in the marked rectangular area as shown in Figure 3 can be analyzed quantitatively. Obtained results are also shown in Figure 4.

After exposure of the initial concrete prisms to 10 freeze-thaw cycles, concrete slices were cut off at different distances from the surface of the damaged specimens as described above. The process of water penetration into

these samples was then measured. A few selected neutron images are shown in Figure 5 for the three different slices. It can be seen that in comparison with results shown in Figure 4 water penetrates deeper into the frost damaged concrete at the same time of contact. Quite obviously freeze-thaw damage increased the rate of water absorption into concrete. This has been observed by Yang et al. (2006) before. The corresponding water distribution profiles in different layers from the surface to centre of concrete were calculated and the resulting profiles are shown in Figure 5. It can be clearly seen that the closer a sample was positioned to the concrete surface, the deeper water penetrates. This is a clear indication that there exists a damage gradient. And damage decreases with increasing distance from the surface.

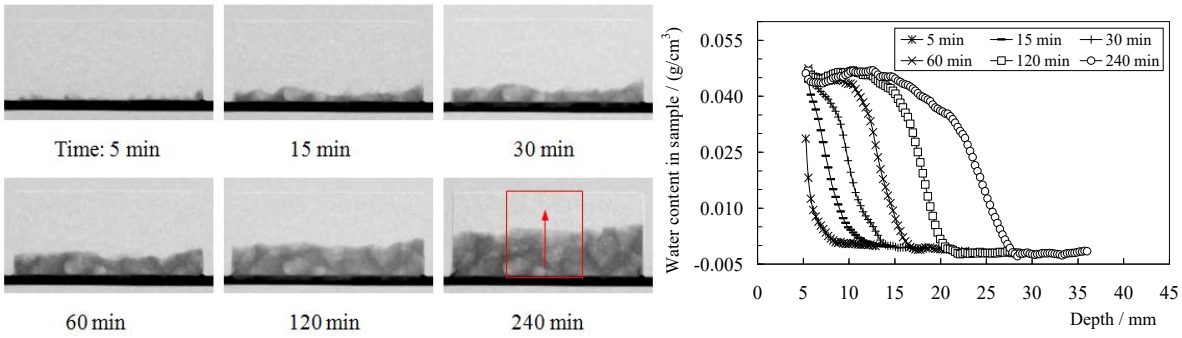

Figure 4 Neutron images of water penetration into neat concrete without air entrainment before frost damage after different durations of contact with water and the corresponding moisture distribution in concrete

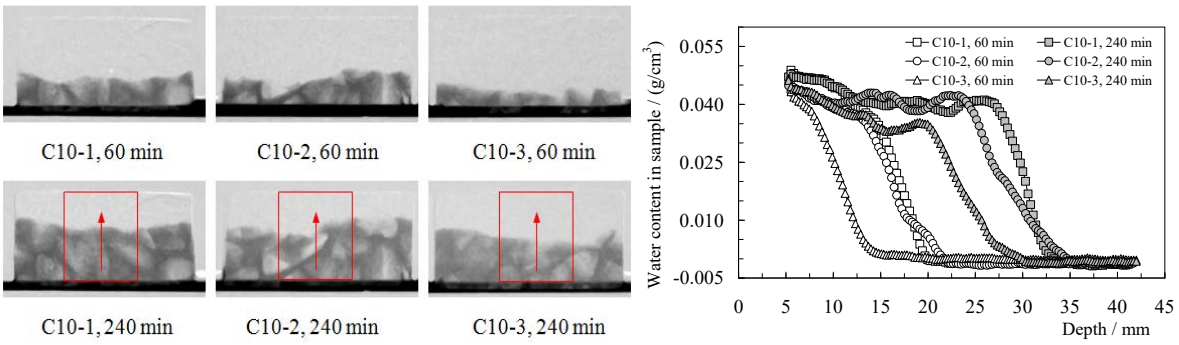

Figure 5 Water penetration into layers of concrete C, having different distances from the surface, after 10 freeze-thaw cycles after 60 and 240 minutes of contact with water, and the moisture distributions.

Water Penetration into Air Entrained Concrete after Frost Damaged

Direct observation of water penetration into concrete prepared with air entraining agent by neutron radiography is shown in Figure 6. The resulting moisture profiles are shown next to the images in Figure 6. The water front moves into this type of concrete with slightly lower rate as compared with normal concrete (see Figure 4). This tendency has been observed before by ordinary capillary suction tests and it can be explained by the fact that the artificially introduced spherical air pores break the capillary force locally. The artificial air pores will be filled with water very slowly and this is probably the reason why we observe two levels of water content in the distribution curves. The pores, which remain empty for a long time even if concrete is in contact with water, assure increased frost resistance. Water in the smaller pores in hardened cement paste around the comparatively big artificial pores is under high capillary under-pressure and therefore it cannot enter the bigger spherical pores.

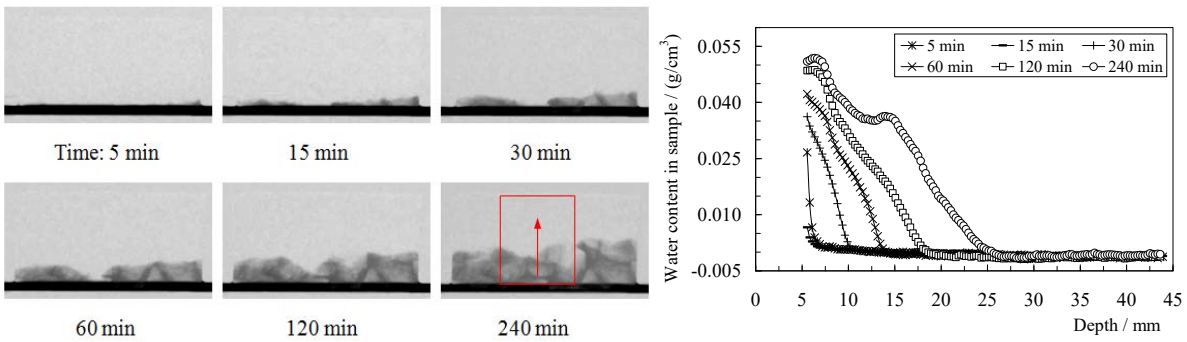

Figure 6 Water penetration into air trained concrete before frost damage and the corresponding moisture distributions in concrete

In a similar way, we followed the process of water penetration into different layers of concrete type CA after 50 and 200 freeze-thaw cycles by neutron radiography. Selected neutron images are shown in Figure 7 and Figure 8 for 50 and 200 freeze-thaw cycles respectively. If we compare these results with those obtained on concrete type C without air entrainment after 10 frost cycles (see Figure 5), it can be seen that concrete type CA absorbs after 50 and 200 freeze-thaw cycles less water than concrete type C after 10 cycles. This indicates the high efficiency of air entrainment to improve frost resistance of concrete. In addition, compared with results obtained on concrete type CA without frost damage (see Figure 6), there is no obvious difference observed on concrete type CA after frost action, with the exception of sample CA200-1. This means that air entraining improves frost resistance significantly but in long lasting contact with water and under a high number of freeze-thaw cycles concrete eventually will be damaged. Under these conditions more rigorous protective measures will be needed.

The obtained digital images on concrete type CA after 50 and 200 freeze-thaw cycles were also evaluated. Detailed evaluation provides us with quantitative moisture distributions. Results along the vertical direction of the rectangular area marked in the images are shown in the right of Figure 9. Water profiles measured in concrete type CA from the surface to the centre after 50 freeze-thaw cycles are nearly the same as results found in specimens without frost action. Even after 200 freeze-thaw cycles, water profiles have not strongly increased except for the surface near layer.

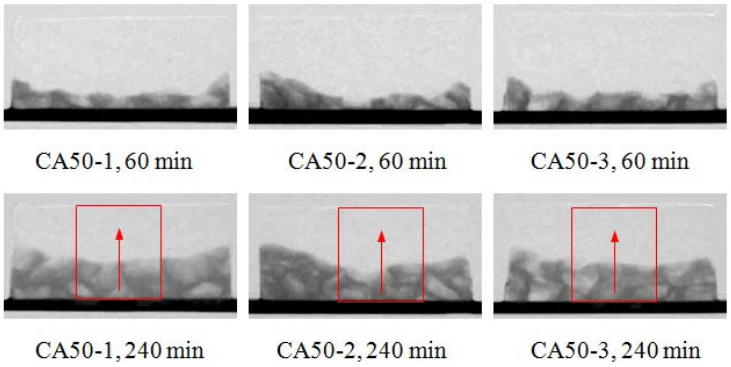

Figure 7 Water penetration into layers of concrete CA, having different distances from the surface, after 50 freeze-thaw cycles

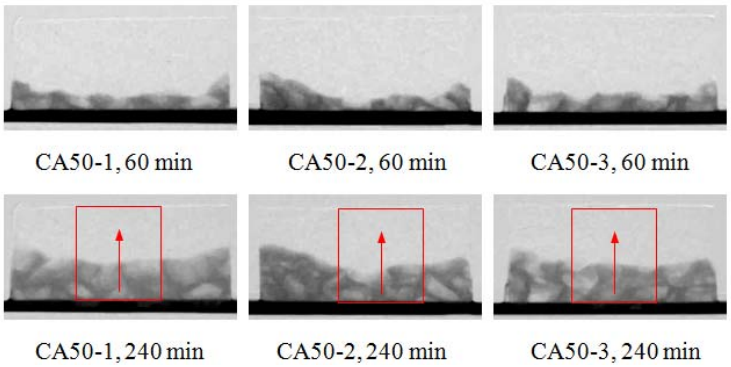

Figure 8 Water penetration into layers of concrete CA, having different distances from the surface, after 200 freeze-thaw cycles

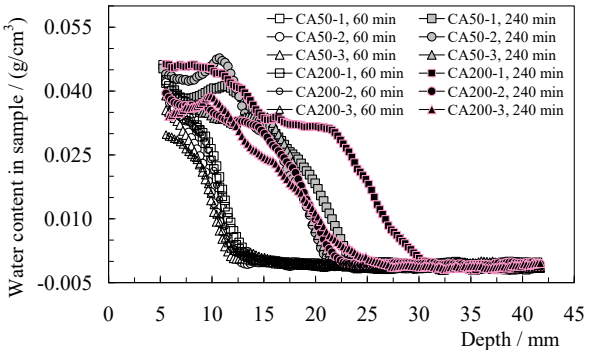

Figure 9 Moisture profiles in layers of concrete CA, having different distances from the surface, after 50 and 200 freeze-thaw cycles after 60 and 240 minutes of contact with water.

CONCLUSIONS

Investigations into the water penetration into undamaged and frost damaged concrete by eutron radiography are described in this paper. Based on the results obtained, the following conclusions can be made: (1) Water penetration into ordinary concrete is increased significantly by frost damage. From the surface to the centre of the tested concrete samples, the rate of water penetration decreases. A damage gradient can be observed. (2) After 50 freeze-thaw cycles, water penetration into air entrained concrete did not vary significantly as compared to values obtained on undamaged concrete. After 200 freeze-thaw cycles, however, the surface near zone absorbed more water although the dynamic elastic modulus as measured on the bulk material has not decreased. Damage concentrated into a thin surface near layer. (3) In addition to the common frost damage induced by freezing of water in narrow gaps and in nano-pores, differential deformations between hardened cement paste and aggregates may also induce damage into the interfaces.

ACKNOWLEDGMENTS

The authors would like to thank Mr. P. Vontobel and Mr. J. Hovind who work in Neutron Imaging & Activation Group, Paul Scherrer Institute (PSI), Switzerland, for the valuable help for operating neutron radiography. Financial supports of ongoing projects by National Basic Research Program of China (no. 2015CB655100) and National Natural Science Foundation of China (nos. 51420105015, 51278260) are also gratefully acknowledged.

REFERENCES

Abd, A. El, Czachor, A. and Milczarek, J. (2009). "Neutron radiography determination of water diffusivity in fired clay brick." *Applied Radiation and Isotopes*, 67(4), 556-559.

Aldea, C. -M., Shah, S. P., and Karr, A. F. (1999). "Permeability of cracked concrete." *Materials and Structures*, 32(6), 370-376.

Cnudde, V., Dierick, M., Vlassenbroeck, J., Masschaele, B., Lehmann, E., Jacobs, P. and Hoorebeke, L. V. (2008). "High-speed neutron radiography for monitoring the water absorption by capillarity in porous materials." *Nuclear Instruments and Methods in Physics Research Section B*, 266(1), 155-163.

Hassanein, R., Meyer, H. O., Carminati, A., Estermann, M., Lehmann, E. H. and Vontobel, P. (2006). "Investigation of water imbibition in porous stone by thermal neutron radiography." *Journal of Physics D: Applied Physics*, 39(19), 4284-4291.

Jacobsen, S., Marchand, J. and Boisvert, L. (1996). "Effect of cracking and healing on chloride transport in OPC concrete." *Cement and Concrete Research*, 26(6), 869-881.

Kanematsu, M., Maruyama, I., Noguchi, T., Iikura, H. and Tsuchiya N. (2009). "Quantification of water penetration into concrete through cracks by neutron radiography." *Nuclear Instruments and Methods in Physics Research Section A*, 605(1-2), 154-158.

Kato, E., Kato, Y. and Uomoto, T. (2005). "Development of simulation model of chloride ion transportation in cracked concrete." *Journal of Advanced Concrete Technology*, 3(1), 85-94.

Lehmann, E. H., Kuhne, G., Vontobel, P. and Frei, G. (2002). "The NEUTRA and NCR radiography stations at SINQ as user facilities for science and industry." *In*: P. Chirco and R. Rosa, Eds. *Proc. 7th World Conference of Neutron Radiography*, Rome, Italy, Aedificatio Publishers, 593-602.

MOHURD. (2010). "Test methods of long-term properties and durability of ordinary concrete." Beijing: Ministry of Housing and Urban-Rural Development of China.

Picandet, V., Khelidj, A. and Bellegou H. (2009). "Crack effects on gas and water permeability of concretes." *Cement and Concrete Research*, 39(6), 537-547.

Pleinert, H., Sadouki, H. and Wittmann, F. H. (1998b). “Determination of moisture distributions in porous building materials by neutron transmission analysis.” *Materials and Structures*, 31(4), 218-224.
Wang, L. C., Soda, M. and Ueda, T. (2008). “Simulation of chloride diffusivity for cracked concrete based RBSM and truss network model.” *Journal of Advanced Concrete Technology*, 6(1), 143-155.
Win, P. P., Watanabe, M. and Machida, A. (2004). “Penetration profile of chloride ion in cracked reinforced concrete.” *Cement and Concrete Research*, 34 (7), 1073-1079.
Yang, Z. F., Weiss, W. J. and Olek, J. (2006). “Water transport in concrete damaged by tensile loading and freeze-thaw cycling.” *Journal of Materials in Civil Engineering*, 18(3), 424-434.
Zhang, P., Wittmann, F. H., Zhao, T. J., Lehmann, E., Vontobel, P. and Hartmann, S. (2009). “Observation of water penetration into water repellent and cracked cement-based materials by means of neutron radiography.” *Int. J. Restoration of Buildings and Monuments*, 15(2), 91-100.
Zhang, P., Wittmann, F. H., Zhao, T. J. and Lehmann, E. H. (2010). “Neutron imaging of water penetration into cracked steel reinforced concrete.” *Physica B: Condensed Matte*r, 405(7), 1866-1871.